THE SIMULATION OF THE ELECTRON CLOUD INSTABILITY IN BEPCII AND CSNS/RCS*

Y. D. Liu#, N. Wang
Institute of High Energy Physics, CAS, P.O. Box 918, 100049, Beijing, China

Abstract

Electron Cloud Instability (ECI) may take place in any positively charged particle circular accelerator especially in positron and proton storage rings. This instability has been confirmed to be a serious restriction to the beam stabilities. The physical model on the formation of electron cloud in various kinds of magnetic fields was introduced in the first section of the paper. The transverse and longitudinal wake field model to present the interaction between electron cloud and beam were introduced in another section of the paper. As an example, in positron storage in BEPCII and RCS of CSNS, the densities of electron cloud and beam instabilities caused by the accumulated electrons were simulated.

INTRODUCTION

The electron cloud accumulated in the vacuum chamber is usually associated with the transverse coupled bunch instability, bunch blow up and bunch lengthening. Experimental studies and numerical simulation have been developed for these phenomena [1]. Now BEPC has been upgraded to a two-ring collider, namely BEPCII, with electron and positron beams circulating in each separate ring. In its commissioning operation, ECI is much weaker because of many restraining methods used in positron ring. The effects of these restraining methods have been validated. In this paper, the simulation to electron cloud in different restraining conditions was introduced.

CSNS is a proton accelerator facility with consists of a linac and a rapid cycling synchrotron (RCS). Two bunches with a population of $1.88\text{x}10^{13}$ will be accumulated and accelerated in the RCS ring, and the electron-proton instabilities might happen in such high intensity proton ring. The ECI in CSNS/RCS is investigated in the last section. The main parameters of the BEPCII and CSNS/RCS ring are summarized in Table 1 and Table 2, respectively [2].

FORMATION OF ELECTRON CLOUD IN BEPCII AND CSNS/RCS

Electrons sourced from the (1) photoelectrons arising from the synchrotron radiation hitting the wall of the vacuum chamber, and (2) secondary emission from electrons hitting the walls, are attracted by the beam electric field and accumulate around the positron beam. Photoelectrons are produced in the chamber and antechamber by the photons hitting the wall with yield rate Y~0.1 and reflectivity R~0.1. If there is photon absorber, the Y and R become as small as Y~0.02, R~0.1.

Table 1: Parameters of the BEPCII

Parameters	Value
Beam energy E(GeV)	1.89
Bunch population $N_b(10^{10})$	4.84
Bunch spacing L_{sep}(m)	2.4
Bunch number n	93
Average bunch length σ_z(m)	0.015
Average bunch sizes $\sigma_{x,y}$(mm)	1.18,0.15
Chamber half dimensions $h_{x,y}$(mm)	60,27
Synchrotron tune Q_s	0.033
Tune $Q_{x,y}$	6.53,7.58
Circumference C(km)	0.237
Average beta function $<\beta>$(m)	10

Table 2: Parameters of the CSNS/RCS

Parameters	Symbol, unit	Value
Inj./Ext. Energy	Ein/Eext, GeV	0.08/1.6
Circumference	C, m	248
Bunch population	N_p, $\times 10^{12}$	9.4
Harmonic number	H	2
Repetition freq.	f_0, H_z	25
Betatron tune	ν_x/ν_y	5.86/5.78
Beam pipe radii	a/b, cm	10
Proton loss rate	P_{loss}, turn^{-1}	1.33×10^{-4}
Proton e– yield	Y_p, e–/p/loss	100
Ionization e–	Y_i, e–/p/loss	1.31×10^{-5}

The percentage of photoelectron escaping out of the antechamber depends on the width of antechamber. In the simulation the beam field is presented by B-E formula and the numerical solver of Poisson-Superfish in the central region of $(10\sigma_x,10\sigma_y)$ and out of this region, respectively. In the simulation we assume that secondary electrons yield (SEY) with and without TiN coating in the chamber is 1.06 and 1.8, respectively.

Simulation results show that the EC density can be reduced by about: 5x if the antechamber is adopted, 6x if the TiN is coated only, 3x if the photon absorber is made in the wall of the chamber only, and 5x if the electrode is installed in the beam chamber. In BEPCII, the antechamber, the photon absorber, and the TiN coating approaches have been adopted. With these three effects taken into account in the simulation, the electron density will be decreased about 80 times, i.e., from $1.1\text{x}10^{13}$ m^{-3} in the case without any restraining method to $1.3\text{x}10^{11}$m^{-3},

*Work supported by National Natural Science Foundation of China (10605032)
#liuyd@mail.ihep.ac.cn

which is lower than the threshold causing the strong head-tail instability as described in later sections.

Figure 1 shows the electron cloud distribution in the vacuum chamber with different transverse shapes with or without electrodes.

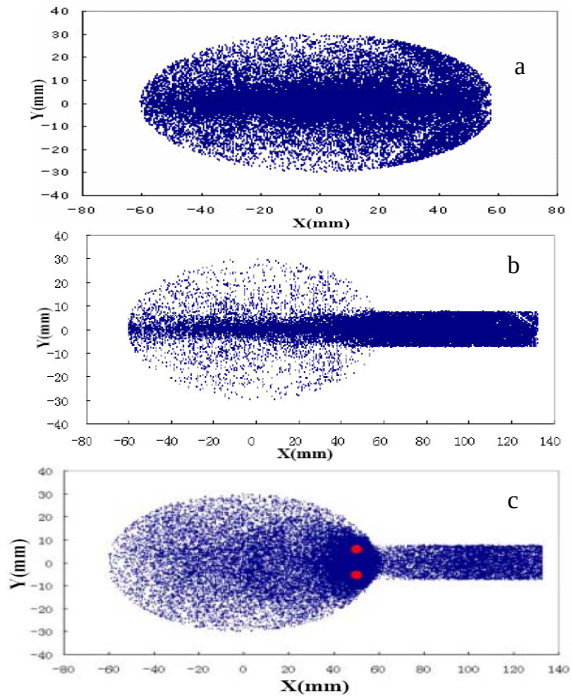

Figure 1: The EC distribution in vacuum chamber (a; elliptic pipe; b: antechamber pipe; c: antechamber with electrodes).

In the above simulation, we don't consider the effect of magnetic fields including dipole, quadrupole, sextupole and solenoid fields. In the region of dipole magnetic field without considering the fringe field, the magnetic field is only in vertical direction, $B=B_y$. For a quadrupole magnetic field, $\boldsymbol{B}$ can be expressed by

$$B_x = k_1 y,$$
$$B_y = k_1 x,$$
$$k_1 = \frac{1}{B\rho}\frac{\partial B_y}{\partial x}, \quad (1)$$

where $B\rho$ is magnetic rigidity. For a sextupole magnetic field, $\boldsymbol{B}$ can be expressed by

$$B_x = k_2 xy,$$
$$B_y = \frac{1}{2}k_2(x^2 - y^2),$$
$$k_2 = \frac{1}{B\rho}\frac{\partial^2 B_y}{\partial x^2}, \quad (2)$$

In uniform solenoid field, the magnetic field is only in longitudinal direction, $B=B_z$.

According to the simulation in Figure 2, it is clear that in the magnetic fields, the electron cloud density is much lower than the density in drift region. The uniform solenoid field is the most effective way to confine the photoelectrons. All of the photoelectrons are confined to the vicinity of the vacuum chamber wall. So in the positron ring of BEPCII, the solenoid has been winded on the vacuum chamber of straight section and the magnetic field designed to be 30 gauss, which will be enough to clear the electron cloud in the central region.

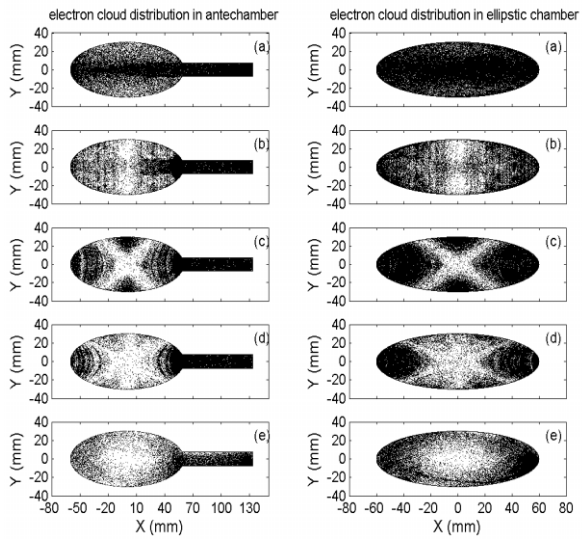

Figure 2. Distribution of electron cloud in various kinds of magnetic field (left: antechamber chamber; right: elliptic chamber; a: free field region; b: dipole field; c: quadrupole field; d: sextupole field; e: solenoid field Bz=10 G).

In CSNS/RCS, the photoelectron effects are much smaller. So there are three candidate mechanisms of electron production considered in this article, including: lost protons hitting the chamber wall, electrons produced by residual gas ionization, and secondary electron emission.

The electron yield due to residual gas ionization is determined by the ionization cross section and the vacuum pressure in the beam chamber. Residual gases of CO and H_2 are considered, whose ionization cross sections are $\sigma(CO)$=1.3x10^{22}m^2 and $\sigma(H_2)$=0.3x10^{22} m^2. The corresponding electron yield at vacuum pressure p=10 nTorr and room temperature (T = 294 K) is 1.22x10^5 e/p/turn. The electrons are produced along the beam trajectory.

The mechanism of electron yield due to proton loss is not yet well known. In the simulation, we use the simple model proposed by Furman et al [3], that the number of electrons generated by lost protons hitting the vacuum chamber wall is $N_p x Y x p_{loss}$, per turn for the whole ring, where Y is the effective electron yield per lost proton, and p_{loss} is the proton loss rate per turn per beam particle. According to the beam loss tracking simulation of the

RCS ring, a total beam loss of 6% mostly occurs in the collimation region during the first 1 ms. by using the assumption of 100 e/p/loss, we obtain an electron production rate of $1.16\text{x}10^{2}$ per turn, which is 3 orders higher than that of gas ionization. We assume the lost proton time distribution to be proportional to the longitudinal bunch intensity.

In the simulation, the electrons are simulated by macro particles. We use 1000 macro-particles to represent primary electrons generated when each bunch slice passes through the electron region. The secondary electron emission occurs when the particles hit on the beam chamber wall. The macro-electrons are tracked dynamically in the transverse plane. The space charge force is computed by the PIC method and applied to particles at each slice in the bunch and each step in the gap. The motion of macro-electrons and macro-protons are tracked during the EC region. After that, the bunch is transformed according to the six-dimensional linear equation. Figure 3 shows the building progress of the electron cloud in RCS with different proton loss. The results show maximum electron density at the bunch tail, and the electron density keep almost unchanged at the bunch head.

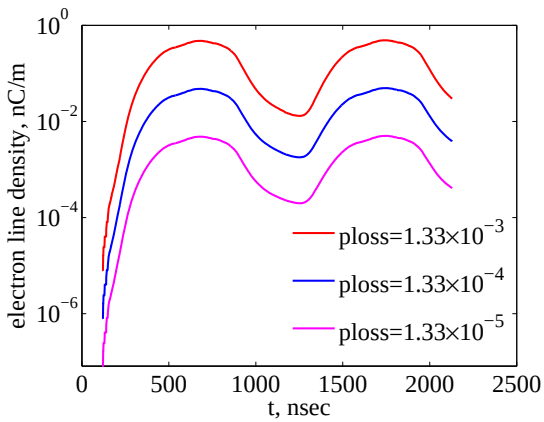

Figure 3: The density of EC for different proton losses.

THE TRANSVERSE AND LONGITUDINAL INSTABILITY CAUSED BY THE ELECTRON CLOUD

In the simulation to the coupled bunch instability, a bunch is expressed as a macro-particle and the EC can be represented by macro-particles. The force between the bunch and electron is represented by the Bassetti-Erskine formula and the solver of Poisson-Superfish in the central region of $(10\sigma_x, 10\sigma_y)$ and out of the region, respectively. By tracking the motion of the bunch and the formation of the EC in the same time, the oscillation amplitudes of 93 bunches and the EC density are recorded. The growth time can be obtained by fitting the amplitude of the oscillation. From the previous results, without any restraining methods the EC density is $1.03\times10^{13}\text{m}^{-3}$, but when using the antechamber, photon absorber and TiN coating, the density will be decrease to 1.35×10^{11} m^{-3}. In these two conditions we track the coupled bunches oscillation in vertical direction, obtaining the growth time τ_{1y}~0.08ms and τ_{2y} ~4.3ms. The Growth behavior of the coupled bunch oscillation and the sideband spectra are shown in Figure 4.

Based on the head-tail model, a code was developed to simulate the beam size blow up. In the model, concentrating electron cloud at one location s of the ring, the EC and the bunch are represented by N_e and N_p macro- particles with transverse uniform and Gaussian distributions, respectively. We use vectors (x_e, x_e') and (y_e, y_e') to describe the transverse motion of electron respectively, without considering the longitudinal force imposed by the EC. The particle's synchrotron oscillation in a bunch being included, the motion of bunch macro-particles are described by the 3D vector, $(x_p, x_p', y_p, y_p', z, \frac{\Delta P}{P})$. The bunch is divided into N_s slices, which interact with the EC one another and cause the distortion of the EC distribution. The macro-particles in different slices can change their positions as the synchrotron oscillation occurs.

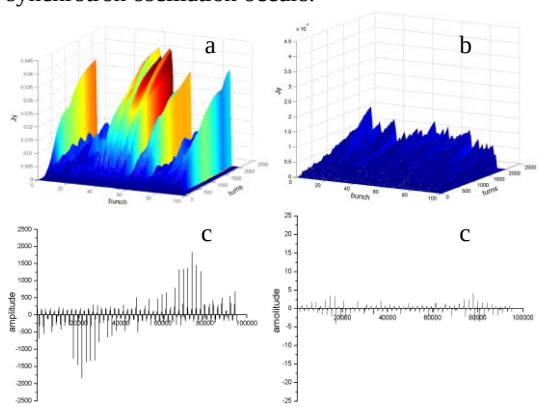

Figure 4: Growth behavior of coupled-bunch oscillation (Tracking result: a and b; sideband spectra: c and d).

After tracking the motions of bunch macro-particles for 4096 turns in the different EC densities, we find that the threshold by simulation is comparable to the analysis result. The tracking results are shown in Figure 5. It is clear that the threshold of the blow up of electron cloud is about 1.0×10^{12} m^{-3}.

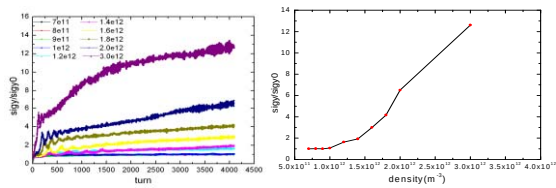

Figure 5: Beam vertical size in the different EC densities.

The same method was used to calculate the transverse bunch oscillation in RCS. There we include the RF acceleration progress.

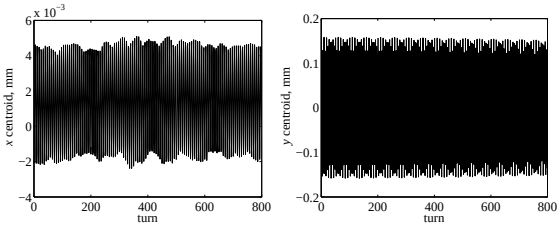

Figure 6: Bunch transverse RMS in RCS.

On the other hand, the positron bunches have to lose some mount of their kinetic energy to build the electron cloud during the interaction with the electrons. The energy variation inside the bunch can be seen as a longitudinal wake. The bunch particles have an additional energy spread due to the longitudinal wake from the electron cloud. the longitudinal electric field of the electron cloud is expressed as,[4]

$$E_z = Z_0 \int_r^a j_r dr, \tag{3}$$

where Z_0 the impedance in free space and j_r is transverse current density of electron cloud.

As an example of BEPCII, assuming the bunch current is 9.8mA, the electric field caused by different electron cloud density is shown in Figure 7.

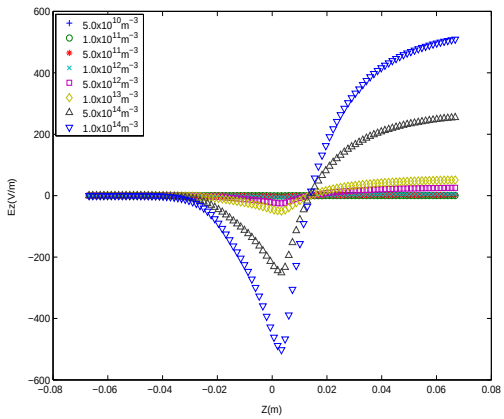

Figure 7: Longitudinal electric fields for different electron cloud densities.

The bunch length and energy spread varied due to the longitudinal wake caused by the electron cloud. The longitudinal interaction between bunch and electron cloud depends on the bunch current and density of electron cloud. A normal method to simulate the process of bunch lengthening is to track the motions of many macro-particles presenting the bunch. The motion of macro-particles is described in the longitudinal phase by [5]

$$z_i(n) = z_i(n-1) + \frac{\alpha c T_0}{E}\varepsilon_i(n) \tag{4}$$

$$\varepsilon_i(n) = \varepsilon_i(n-1) - \frac{2T_0}{\tau_\varepsilon}\varepsilon_i(n-1) + 2\sigma_{\varepsilon 0}\sqrt{\frac{T_0}{\tau_\varepsilon}}R_i(n) - U_0 + V\cos(\phi_s + \frac{2\pi h}{C}z_i(n)) + V_i[z_i(n))]. \tag{5}$$

where $\varepsilon_i(n)$ and $z_i(n)$ are the energy and position coordinates of the i^{th} particle after n revolutions in the storage ring. T_0 is the revolution period; τ_ε the damping time; U_0 the energy lost per turn; ϕ_s the synchronous phase; h the harmonic number; C the ring circumference; E the bunch energy; α the momentum compaction factor; $\sigma_{\varepsilon 0}$ the natural energy spread; R_i a random number obtained from a normal distribution with mean 0 and RMS 1. The wake potential V_i caused by the electron cloud depends on the longitudinal electric field of E_z.

In the simulations 10^6 macro-particles are tracked over 6 longitudinal damping times and the bunch length are calculated by averaging particle positions in the last damping time. For BEPCII, positron bunch current 9.8mA, bunch natural length 13.53mm, the longitudinal electric field and the tracking result for bunch length in different electron cloud density are shown in Figure 8.

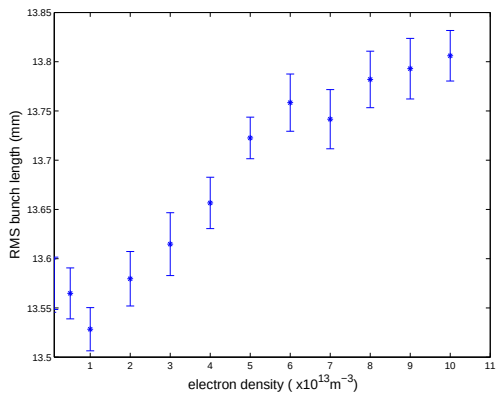

Figure 8: Bunch length for different electron densities.

Synchrotron tune shift is reduced about 5% of the undisturbed tune with the electron cloud density of $1.0\text{x}10^{14}\text{m}^{-3}$, as shown in Figure 9. The longitudinal action between electron cloud and bunch can be seen as an electron cloud potential well, which causes the possible bunch distortion.

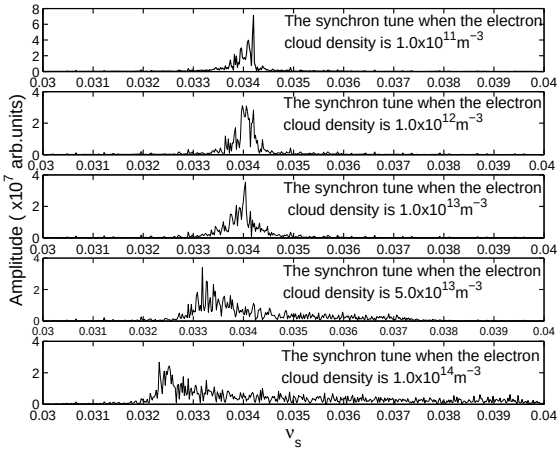

Figure 9: Synchrotron tune shift by the electron cloud.

According to the simulation results for bunch length in different electron cloud density, the electric field due to electron cloud can lead to the bunch lengthening. The bunch initial Gaussian distribution is shifted slightly in the forward direction for compensating the additional energy loss to the electron cloud. The longitudinal action between electron cloud and bunch can be seen as an electron cloud potential well which cause the possible bunch distortion.

CONCLUSION

With simulation, the efficiency for antechamber with photon absorber, TiN coating and clearing electrode to reduce the EC density is explored. All of these results are very meaningful for understanding the mechanism, as needed for the design and operation of storage rings for factory-like colliders. Particularly we have decided to adopt antechamber with photon absorber and TiN coating in the BEPCII to cure the ECI. The EC density can be suppressed to below the threshold of strong head-tail like instability, while the coupled bunch instability can be damped with feedback system. The longitudinal effect of electron cloud serves as a potential well to interact the dynamics of bunch particles. Tracking methods to simulate the bunch length in different electron cloud density show that the bunch lengthening caused by the electron cloud density $1.0x10^{14}m^{-3}$, is just 2.0% of the natural bunch length. Its effect appears to be negligible for BEPCII.

ACKNOWLEDGEMENTS

The author is grateful for the suggestions from the members of accelerator physics group in IHEP and KEK.

REFERENCES

[1] K. Ohmi, F. Zimmermann, “Head-tail Instability caused by Electron Cloud in Positron Storing Rings”, Phys. Rev. Lett. 85, 3821(2000).

[2] WEI Jie, FU Shi-Nian, FANG Shou-Xian et al. China Spallation Neutron Source Accelerators: Design, Research, andDevelopment. In: C. Biscari et al. Proceedings of EPAC'06.Edinburgh, Scotland: EPS-AG, 2006. 366-368.

[3] Furman M A, Pivi M. Simulation Results for the Electron Cloud at the PSR. In: Lucas P, Webber S. Proceedings of PAC'01. Chicago, U.S.A.: IEEE, Inc, 2001. 707-709.

[4] A. Novokhatski, J. Seeman, “Simulation of electron cloud multipacting in solenoidal magnetic field”, SLAC-PUB-10327.

[5] R. Siemann, "Computer Simulation of Bunch Lengthening in SPEAR", NIM 203 (1982).